The Astrophysical Journal, 685: L129–L132, 2008 October 1

PROTON-RICH NUCLEAR STATISTICAL EQUILIBRIUM

I. R. Seitenzahl,[1,2,3] F. X. Timmes,[2,4] A. Marin-Laflèche,[5,6] E. Brown,[2,7] G. Magkotsios,[2,8] and J. Truran[2,3,5,9]

Received 2008 July 8; accepted 2008 August 14; published 2008 September 5

ABSTRACT

Proton-rich material in a state of nuclear statistical equilibrium (NSE) is one of the least studied regimes of nucleosynthesis. One reason for this is that after hydrogen burning, stellar evolution proceeds at conditions of an equal number of neutrons and protons or at a slight degree of neutron-richness. Proton-rich nucleosynthesis in stars tends to occur only when hydrogen-rich material that accretes onto a white dwarf or a neutron star explodes, or when neutrino interactions in the winds from a nascent proto–neutron star or collapsar disk drive the matter proton-rich prior to or during the nucleosynthesis. In this Letter we solve the NSE equations for a range of proton-rich thermodynamic conditions. We show that cold proton-rich NSE is qualitatively different from neutron-rich NSE. Instead of being dominated by the Fe-peak nuclei with the largest binding energy per nucleon that have a proton-to-nucleon ratio close to the prescribed electron fraction, NSE for proton-rich material near freezeout temperature is mainly composed of ^{56}Ni and free protons. Previous results of nuclear reaction network calculations rely on this nonintuitive high-proton abundance, which this Letter explains. We show how the differences and especially the large fraction of free protons arises from the minimization of the free energy as a result of a delicate competition between the entropy and nuclear binding energy.

Subject heading: nuclear reactions, nucleosynthesis, abundances

1. INTRODUCTION

Recently, a new nucleosynthesis process was invented to explain the production of the proton-rich isotopes ^{92,94}Mo and ^{96,98}Ru (Fröhlich et al. 2006). In this so-called νp-process, matter ejected from the surface layers of a proto–neutron star is exposed to a strong neutrino flux which results in the following weak interactions:

$$\nu_e + n \rightleftharpoons p + e^-, \tag{1}$$

$$\bar{\nu}_e + p \rightleftharpoons n + e^+. \tag{2}$$

The mass difference between the neutron and the proton causes the neutrino interactions to be dominated by the forward reaction of equation (1), which drives the nuclear matter proton-rich. The matter then expands and assembles into NSE, which is not only proton-rich (i.e., $Y_e > 0.5$) but actually contains a large mass fraction of free protons. The forward reaction of equation (2) converts some of the free protons to neutrons, which allows nuclear matter to move past the "bottle neck" nucleus ^{64}Ge via the fast ^{64}Ge$(n,p)^{64}$Ga reaction, and the aforementioned proton-rich isotopes are synthesized during the freezeout phase from the proton-rich NSE state (Fröhlich et al. 2006). Meyer (1994), Jordan & Meyer (2004), Pruet et al. (2005, 2006), and Wanajo (2006) calculate nucleosynthesis in similar environments.

We show that the NSE mass fractions exhibit a great degree of symmetry across the line $Y_e = 0.5$ for high temperatures where the composition is dominated by free nucleons and ^{4}He. For colder temperatures ($T_9 \leq 6.0$ and $\rho \sim 10^7$ g cm^{-3}), there are hardly any free neutrons present in the NSE state for $0.4 < Y_e \leq 0.5$. A naïve guess based on symmetry of NSE abundances would therefore not lead one to expect many free protons during freezeout for $Y_e > 0.5$ either. A large number of free protons is however observed to occur in nuclear reaction networks calculations. We show that for a relatively cold, near freezeout temperature NSE state, there is indeed a qualitative difference in the mass fraction trends for $Y_e > 0.5$ and $Y_e < 0.5$. Restricting ourselves to the Ni isotopic chain and free nucleons, we explain how this difference arises as a result of a competition between the temperature-dependent entropy term and the nuclear binding energy term contribution to the free energy.

2. NUCLEAR STATISTICAL EQUILIBRIUM EQUATIONS

NSE is established if all fusion reactions are in equilibrium with their inverses for a set of thermodynamic-state variables and Y_e (e.g., Clifford & Tayler 1965). Detailed balance relates the chemical potential of a nucleus $^{Z_i+N_i}_{Z_i}X_i$ to those of free nucleons: $\mu_i = Z_i\mu_p + N_i\mu_n$. This yields an expression for the number density of nucleus i:

$$n_i = g_i \left(\frac{2\pi m_i kT}{h^2}\right)^{3/2} \exp\left[\frac{Z_i(\mu_p^{\rm kin} + \mu_p^{\rm C}) + N_i\mu_n^{\rm kin} - \mu_i^{\rm C} + Q_i}{kT}\right].$$

The NSE constraint equations can be perhaps most naturally written in a number density basis as $\sum_i A_i n_i = n_B$ and $\sum_i Z_i n_i = n_B Y_e$, where $n_B = n_n + n_p$ and $Y_e = n_p/n_n$. We solve the NSE constraint equations numerically for the kinetic chemical potentials $\mu_p^{\rm kin}$ and $\mu_n^{\rm kin}$ of the (assumed Maxwellian) protons and neutrons, respectively. For the Coulomb contributions $\mu_p^{\rm C}$ and $\mu_i^{\rm C}$ and the nuclear partition functions g_i we use the same formalism as Calder et al. (2007) and Seitenzahl et al. (2008).

[1] Department of Physics, University of Chicago, Chicago, IL 60637.
[2] Joint Institute for Nuclear Astrophysics (JINA).
[3] Enrico Fermi Institute, University of Chicago, Chicago, IL 60637.
[4] School of Earth and Space Exploration, Arizona State University, Tempe, AZ 85287.
[5] Department of Astronomy and Astrophysics, University of Chicago, Chicago, IL 60637.
[6] Department of Physics and Astronomy, École Polytechnique, Palaiseau, France.
[7] Department of Physics and Astronomy, Michigan State University, East Lansing, MI 48824.
[8] Department of Physics, University of Notre Dame, Notre Dame, IN 46556.
[9] Argonne National Laboratory, Argonne, IL 60439.

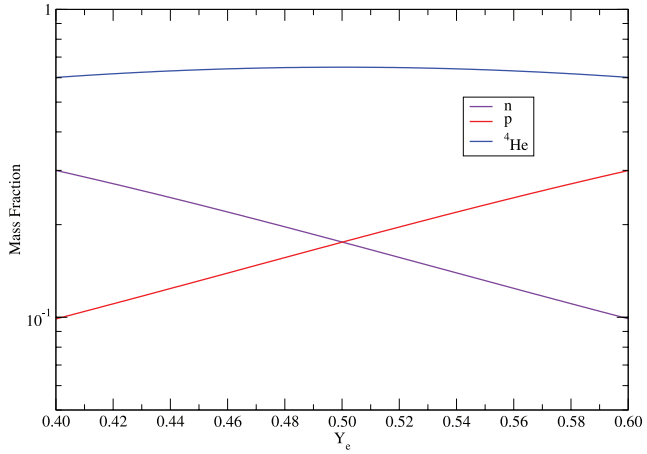

FIG. 1.—Mass fractions of nuclei in NSE as a function of electron fraction for a constant density $\rho = 10^7$ g cm^{-3} ($n_B = 6.0 \times 10^{30}$ cm^{-3}) and relatively high temperature $T = 9.0 \times 10^9$ K. Shown are all nuclei with mass fractions larger than 10^{-2}. The mass fractions exhibit large degree of (in the case of nucleons complementary) symmetry across $Y_e = 0.5$.

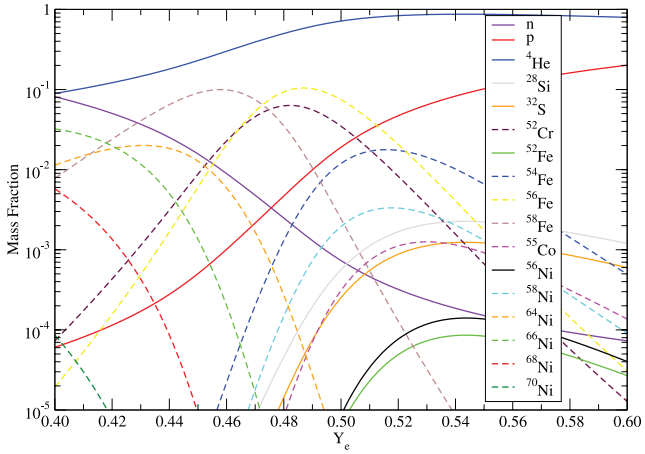

FIG. 2.—Mass fractions of nuclei in NSE as a function of electron fraction for a constant density $\rho = 10^7$ g cm^{-3} ($n_B = 6.0 \times 10^{30}$ cm^{-3}) and temperature $T = 6.5 \times 10^9$ K. Shown are some abundant nuclei with mass fractions larger than 10^{-5}. The symmetry across $Y_e = 0.5$ is already broken.

3. RESULTS

The results presented here are all for a baryonic mass density of $\rho = 10^7$ g cm^{-3}, which corresponds to a baryon number density of $n_B \approx 6.0 \times 10^{30}$ cm^{-3}. At high temperature ($T_9 = 9.0$) the NSE mass fractions are dominated by free nucleons and ^{4}He. The ^{4}He mass fraction is symmetric across the line $Y_e = 0.5$, and the mass fractions of free protons and neutrons are symmetric in a complementary sense—free protons are more abundant for $Y_e > 0.5$ and free neutrons are more abundant for $Y_e < 0.5$ (see Fig. 1).

At somewhat lower temperature ($T_9 = 6.5$), the symmetry of the NSE mass fractions across the line of self-conjugacy is broken and only qualitatively discernible. For $\Delta Y_e > 0$, free neutrons are less abundant for $Y_e = 0.5 - \Delta Y_e$ than are free protons for $Y_e = 0.5 + \Delta Y_e$ (see Fig. 2). Furthermore, the mass fraction of ^{4}He is not symmetric anymore and the abundance peaks of the Fe-peak nuclei are wider on the proton-rich side.

At even lower temperature ($T_9 = 3.5$), the qualitative features of the mass fractions of nuclei in NSE as a function of Y_e at fixed density and temperature change dramatically in the transition from the neutron-rich to the proton-rich side. For $Y_e < 0.5$, the mass fraction landscape is composed of a sequence of overlapping abundance peaks (e.g., Clifford & Tayler 1965; Hartmann et al. 1985; Nadyozhin & Yudin 2004). Fe-peak nuclei with a proton-to-nucleon ratio equal or close to the prescribed Y_e of the ensemble and a large binding energy per nucleon, q/A, are the most abundant nuclei. For $Y_e > 0.5$, the picture changes abruptly (see Fig. 3). The mass fraction distributions of the Fe-peak nuclei are no longer peaked, but rather either slowly rising or falling. ^{56}Ni remains the most abundant nuclear species by mass all the way out past $Y_e = 0.6$. The mass fraction of free protons continues to rise. ^{52}Fe shows a similar trend like ^{56}Ni, albeit at a smaller abundance level. There is only a slow rise in the mass fractions of proton-rich Fe-peak nuclei for increasing Y_e; the abundance peaks for the Fe-peak nuclei with a proton-to-nucleon ratio equal to Y_e that are so prominent on the neutron-rich side are absent.[10]

[10] Various animations of NSE in proton-rich environments may be downloaded from http://cococubed.asu.edu/code_pages/nse.shtml.

4. DISCUSSION

In NSE, the Helmholtz free energy $\mathcal{F} = (U - Q) - TS$ is minimized with respect to the nuclide mass fractions (e.g., Nadyozhin & Yudin 2005). Before we discuss and compare the terms that make up $\mathcal{F}$ for different choices of compositions, it is instructive to review the dependence of q/A on the number of nucleons along an isotopic chain, the attributes of which ultimately are responsible for the lack of symmetry.

4.1. *The Nuclear Binding Energy*

The ratio q/A on the proton-rich side for the Ni isotopic chain decreases rapidly toward proton drip, whereas it gently increases to a maximum at $A_{\max} = 62$ before slowly falling off toward neutron drip (see Fig. 4). Other isotopic chains, such as the one for Fe, look qualitatively very similar. The shape of the q/A-curve can be qualitatively understood by considering

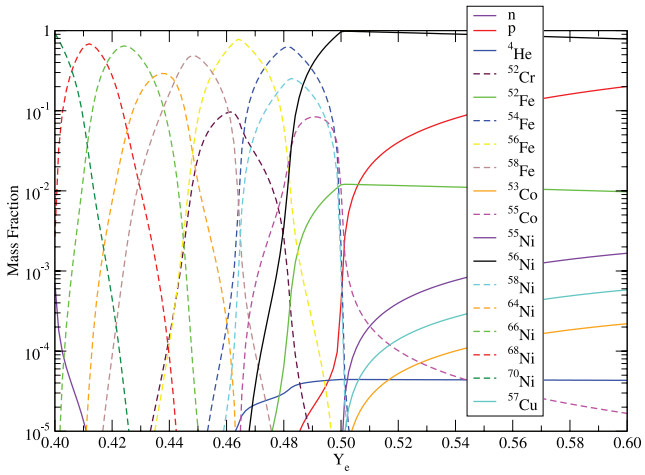

FIG. 3.—Mass fractions of nuclei in NSE as a function of electron fraction for a constant density $\rho = 10^7$ g cm^{-3} ($n_B = 6.0 \times 10^{30}$ cm^{-3}) and temperature $T = 3.5 \times 10^9$ K. Shown are some abundant nuclei with mass fractions larger than 10^{-5}. The mass fractions on either side of $Y_e = 0.5$ exhibit qualitatively very different behavior.

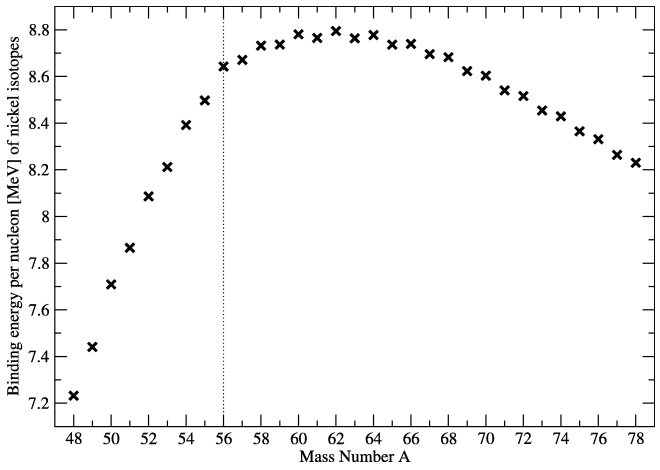

FIG. 4.—Plot of q/A for Ni isotopes. Note the rapid decline on the proton-rich side of ^{56}Ni and the particularly large gap between ^{56}Ni and ^{55}Ni.

a simple liquid-drop mass formula taking the volume, surface, asymmetry, and Coulomb terms into account:

$$Q = a_V - a_S A^{-1/3} - a_A(1 - 2Z/A)^2 - a_C Z^2 A^{-4/3}. \quad (3)$$

For simplicity, we have neglected other terms such as pairing, Wigner, or residual interaction. The derivative with respect to nucleon number is given by

$$\mathcal{S}(A) = \left.\frac{\partial Q}{\partial A}\right|_Z = \frac{a_S}{3}A^{-4/3} + \frac{4a_A Z}{A}\left(1 - \frac{2Z}{A}\right) + \frac{4a_C Z^2}{3}A^{-7/3}. \quad (4)$$

The second (asymmetry) term is positive on the proton-rich side, zero for $2Z = A$, and negative on the neutron-rich side, which gives the q/A-curve its general concave-up shape. It is, however, not entirely symmetric about the line $2Z = A$. In fact, since

$$\left|\frac{Z}{2Z + \Delta A}\left(1 - \frac{2Z}{2Z + \Delta A}\right)\right| < \left|\frac{Z}{2Z - \Delta A}\left(1 - \frac{2Z}{2Z - \Delta A}\right)\right|, \quad (5)$$

the absolute value of the slope due to the asymmetry term alone is larger on the proton-rich side. The first (surface) and third (Coulomb) term are always positive, both monotonically increasing with A, which consequently shifts the most tightly bound isotope to the neutron-rich side and further increases the asymmetry in the slopes on either side of the maximum. This simple argument shows the essence of how the surface and Coulomb terms in the nuclear mass formula leads to a more rapid fall off in q/A on the proton-rich side. ^{56}Ni is doubly magic and a Wigner $N = Z$ nucleus, resulting in an increase in q/A compared to the simple mass formula above and the dominance of ^{56}Ni in cold, proton-rich NSE.

4.2. *Free Energy for Different Compositions*

To get a better understanding of the different low-temperature behavior of abundance trends as a function of Y_e for the proton- and neutron-rich regimes, we consider a simplified system and restrict the composition to nuclides from the Ni isotopic chain and free nucleons. For a concrete example, let us compare two compositions at $Y_e = 28/55 \sim 0.5091$, one consisting of pure ^{55}Ni, and the other consisting of a mix of free protons and a "test" nucleus, here ^{56}Ni (see Fig. 5). The mean binding energy per nucleon is given by $\bar{Q} = \sum_i q_i n_i/n_B$, where q_i is the binding energy of nucleus i and $q_n = q_p = 0$. $\bar{Q}$ of 28 ^{55}Ni nuclei [(28 × 467.352 MeV)/(28 × 55) = 8.497 MeV nucleon^{-1}] is slightly larger than that of 27 ^{56}Ni nuclei plus 28 protons [(27 × 483.992 MeV)/(27 × 56 + 28 × 1) = 8.486 MeV nucleon^{-1}]. NSE, however, favors the state with the lowest $\mathcal{F}$, not the lowest $\bar{Q}$. For $T_9 = 3.5$ and $n_B = 6.0 \times 10^{30}$ cm^{-3} we know that pure ^{55}Ni is disfavored and should have higher $\mathcal{F}$. This is indeed the case, as ΔU between the two states is negligible and the entropy term TS is much larger for the state with the free protons (see Fig. 6), resulting in lower $\mathcal{F}$. It is evident from Figure 5 that with ^{56}Ni as the test nucleus, the increase in the entropy term on the neutron-

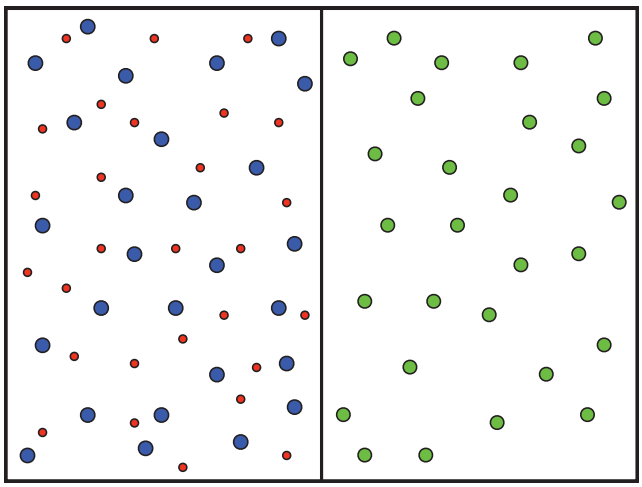

FIG. 5.—*Left*: 27 ^{56}Ni nuclei and 28 protons. *Right*: 28 ^{55}Ni nuclei. Both compositions have identical electron fraction $Y_e = 28/55$. Even though pure ^{55}Ni has a marginally higher $\bar{Q}$, the NSE state at $\rho \sim 10^7$ g cm^{-3} near freezeout is closer to the mix of ^{56}Ni nuclei and protons depicted schematically in the left panel. For almost equal $\bar{Q}$, the composition with more particles and higher entropy is statistically preferred

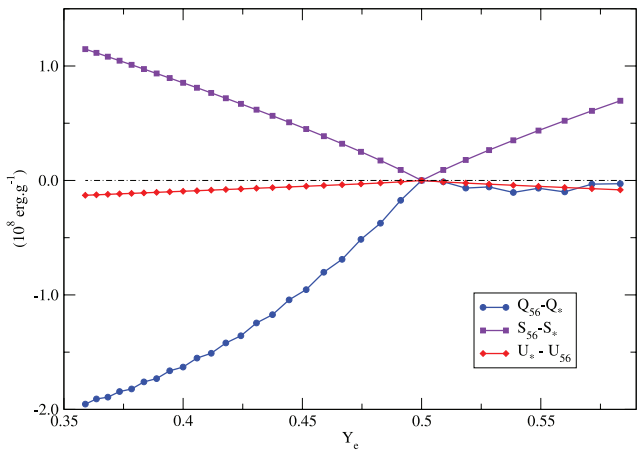

FIG. 6.—Differences in internal energy U, entropy contribution TS, and binding energy Q between a mix of ^{56}Ni (subscript 56) and free protons (for $Y_e > 0.5$) or neutrons (for $Y_e < 0.5$) and a composition of pure Ni isotope (subscript *) for different Y_e.

rich side for the mixed composition is more than compensated by the increase in binding energy by the pure state. On the other hand, for the proton-rich side the $\bar{Q}$ of both compositions is nearly equal, and the higher entropy of the state with more particles makes the difference.

Using the data from the latest atomic mass evaluation of Audi et al. (2003) and an equation of state (Timmes & Arnett 1999; Timmes & Swesty 2000; Fryxell et al. 2000), we compute and compare $\mathcal{F}$ for such compositions for the whole Ni isotopic chain, with each isotope as the test nucleus at a time. If $Y_e < Z/A$ of the test nucleus (in the example above and in Fig. 6 this is ^{56}Ni), we use free neutrons instead of free protons.

For any given Y_e, we can derive $\bar{Q}$ for a mix of a test nucleus ^{A}Ni with the appropriate number of free protons or neutrons,

$$\text{if} \quad \frac{28}{A} < Y_e, \quad \bar{Q} = q(^A\text{Ni})\,\frac{1 - Y_e}{A - 28}, \tag{6}$$

$$\text{if} \quad \frac{28}{A} > Y_e, \quad \bar{Q} = q(^A\text{Ni})\,\frac{Y_e}{28}, \tag{7}$$

where $q(^A\text{Ni})$ is the total binding energy of ^{A}Ni. $\mathcal{F}$ of all such compositions is shown as a function of Y_e in Figure 7, which clearly shows that for $Y_e < 0.5$ a pure composition of the Ni isotope with $Y_e = 28/A$ has the lowest $\mathcal{F}$, and that for $Y_e > 0.5$ a composition consisting of free protons and ^{56}Ni minimizes $\mathcal{F}$. Other choices for the test nucleus have larger $\mathcal{F}$ (dotted lines in Fig. 7).

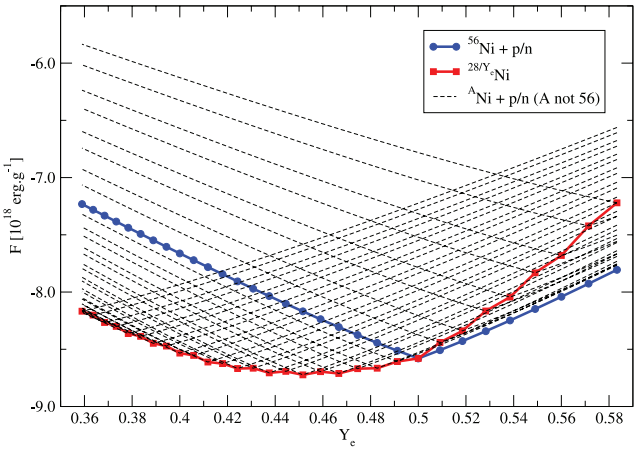

FIG. 7.—Helmholtz free energy $\mathcal{F}$ of compositions consisting of Ni isotopes and nucleons as a function of Y_e. $T = 3.5 \times 10^9$ K and $n_B = 6.0 \times 10^{30}$ cm^{-3}. For $Y_e > 0.5$, a mix of protons and test isotope ^{56}Ni (*thick blue line with dots*) is favored. Other test isotopes (*dotted lines*) result in larger $\mathcal{F}$. For $Y_e < 0.5$, a pure isotope composition (*thick red line with squares*) has the lowest $\mathcal{F}$.

5. CONCLUSIONS

We have presented mass fraction trends for NSE in proton-rich environments. We have explained the, at first sight peculiar, high free proton mass fractions for $Y_e > 0.5$ and large mass fraction of ^{56}Ni even out to $Y_e = 0.6$ by considering a simplified model. Restricting ourselves to the Ni isotopic chain, we have explicitly shown that for $Y_e > 0.5$, $\mathcal{F}$ is minimized by a state consisting of a mixture of free protons and the self-conjugate ^{56}Ni, whereas for $Y_e < 0.5$ a state with a pure composition made up of the Ni isotope that has Z/A closest to the prescribed Y_e is preferred. In reality, other isotopic chains are of course accessible. Other Fe-peak nuclides (especially the slightly neutron-rich even isotopes of Fe) compete with Ni isotopes for the most tightly bound nucleus with Z/A near Y_e (see Fig. 3), giving the familiar NSE abundance pattern.

This work is supported at the University of Chicago by the DoE under grant B523820 to the ASC/Alliances Center for Astrophysical Thermonuclear Flashes, and the NSF under grant PHY 02-16783 for the Frontier Center "Joint Institute for Nuclear Astrophysics" (JINA), and at ANL by the US DoE, Office of Nuclear Physics, under contract DE-AC02-06CH11357. E. F. B. is supported by the NSF under grant AST 05-07456.

REFERENCES

Audi, G., Wapstra, A. H., & Thibault, C. 2003, Nucl. Phys. A, 729, 337
Calder, A. C., et al. 2007, ApJ, 656, 313
Clifford, F., & Tayler, R. 1965, MmRAS, 69, 21
Fröhlich, C., et al. 2006, Phys. Rev. Lett., 96, 142502
Fryxell, B., et al. 2000, ApJS, 131, 273
Hartmann, D., Woosley, S. E., & El Eid, M. F. 1985, ApJ, 297, 837
Jordan, G. C., IV, & Meyer, B. S. 2004, ApJ, 617, L131
Meyer, B. S. 1994, ARA&A, 32, 153
Nadyozhin, D. K., & Yudin, A. V. 2004, Astron. Lett., 30, 634
———. 2005, Astron. Lett., 31, 271
Pruet, J., Hoffman, R. D., Woosley, S. E., Janka, H.-T., & Buras, R. 2006, ApJ, 644, 1028
Pruet, J., Woosley, S. E., Buras, R., Janka, H.-T., & Hoffman, R. D. 2005, ApJ, 623, 325
Seitenzahl, I. R., Townsley, D. M., Peng, F., & Truran, J. T. 2008, At. Data Nucl. Data Tables, in press
Timmes, F. X., & Arnett, D. 1999, ApJS, 125, 277
Timmes, F. X., & Swesty, F. D. 2000, ApJS, 126, 501
Wanajo, S. 2006, ApJ, 647, 1323